

# Neutron spectrum unfolding based on generalized regression neural networks for neutron fluence and neutron ambient dose equivalent estimations

Jie Wang\*, Zhirong Guo, Xianglei Chen, Yulin Zhou

Wuhan Second Ship Design and Research Institute, Wuhan, 430064, China



## ARTICLE INFO

**Keywords:**

Neutron fluence  
Neutron ambient dose equivalent  
Neutron spectrum  
Generalized regression neural networks

## ABSTRACT

Neutron fluence and neutron ambient dose equivalent,  $H^*(10)$ , are important physical quantities for neutron radiation protection and monitoring. They can be deduced from neutron spectrum, which is usually measured by multisphere system with proper unfolding methods. Novel unfolding methods on the basis of artificial intelligence, mainly artificial neural networks (ANNs), have been researched and developed. However, without normalization on network inputs, ANNs can not be applied to accommodate demands of various neutron field measurements for neutron spectrum unfolding in practice, because the neutron spectra for training the ANNs are mostly extracted from IAEA (2001), the integrals of which over neutron energy are unit fluences. Moreover, derived from an unfolded normalized spectrum, the true values of neutron fluence and  $H^*(10)$  are never to know. In this work, three normalization methods—zero-mean normalization method, min-max normalization method, and maximum-divided normalization method were used to process with the inputs of generalized regression neural networks (GRNNs), and a new method was proposed for neutron fluence and  $H^*(10)$  estimations derived from unfolded neutron spectrum based on GRNNs for the first time. Sixty-three neutron spectra were unfolded based on GRNNs with use of three normalization methods, and the corresponding neutron fluences and  $H^*(10)$  were obtained and compared. From the testing results, the GRNNs with the maximum-divided method is most effective to unfold neutron spectrum and to evaluate neutron fluence and  $H^*(10)$ . The feasibility of the method was further studied through experiments by using Bonner sphere spectrometer in well characterized  $^{241}\text{Am}$ -Be neutron field.

## 1. Introduction

Neutron fluence and neutron ambient dose equivalent,  $H^*(10)$ , are of great significance in radiation protection physics (Knoll, 1999), especially,  $H^*(10)$  plays a non trivial role in neutron field measurements for ensuring the personal safety in the staff workplace. In order to estimate  $H^*(10)$ , neutron rem counters and neutron area monitors have been designed and used in practical situations (Vega-Carrillo et al., 2014). They commonly assemble a passive or an active neutron detector inside a polyethylene moderator. The active detector systems with electronics can directly display  $H^*(10)$  rates converted from the detector count rates (Andersson and Braun, 1963; Leake, 1966; Birattari et al., 1990), while the passive detector systems is heavily used in pulsed, mixed and intense neutron fields where the active neutron detectors can not work (Vega-Carrillo et al., 2013). To improve the neutron energy dependent response, multi-counter neutron dose survey instrument embeds multiple neutron detectors or position sensitive

counters inside a single spherical polyethylene moderator, and  $H^*(10)$  rate is a linear combination of count rates given by the corresponding electronics connected to the neutron detectors (Bartlett et al., 1997; Zhou et al., 2013). Alternatively, Neutron spectrometry composed by a multi-element system can be used in a wider energy range with better detection efficiency and can have better dose evaluation performance (Fehrenbacher et al., 1999). Neutron fluence is calculated by integrating unfolded neutron spectrum over neutron energy, and  $H^*(10)$  is through integrating unfolded neutron spectrum with neutron fluence-to-ambient dose equivalent conversion coefficients over neutron energy (Guzman-Garcia et al., 2015).

Bonner sphere spectrometer (BSS), as an appropriate and widely used neutron spectrometry, was first introduced by Bramblett et al. (1960). It consists of a set of high density polyethylene spheres with different diameters, of which a thermal neutron detector is located at the center. However, the BSS cannot measure neutron spectrum without unfolding process. Novel unfolding methods based on artificial

\* Corresponding author.

E-mail address: [1091629887@qq.com](mailto:1091629887@qq.com) (J. Wang).

intelligence, mainly artificial neural networks (ANNs), become of interest to obtain neutron spectrum (Vega-Carrillo et al., 2006, 2007). ANNs are networks modeled on the biological nervous system of the human brain (Bing and Titterington, 1994; Arbib, 2003). As a kind of nonlinear black box model structures, ANNs can link a set of inputs and the corresponding outputs by optimizing the synaptic weights. Here, the knowledge is stored during the training and the learning process. Thus, the stored knowledge is available to give an appropriate output when a new input is presented. For neutron spectrum unfolding application, the inputs are sphere readings and the outputs are neutron spectra (Braga and Dias, 2002; Kardan et al., 2003).

In prior works, three artificial intelligence methods have been optimized and used for neutron spectrum unfolding, generalized regression neural network (GRNN), as a type of artificial neural networks (ANNs), has turned out to be the method with the best unfolding performance (Wang et al., 2019). However, the inputs of ANNs for training (i.e., sphere readings) are commonly calculated using the normalized neutron spectra (i.e., spectra of which the integral over energy is normalized fluences) extracted from the International Atomic Energy Agency compendium (IAEA, 2001) multiplied by response matrix (Vega-Carrillo et al., 2005; Martinez-Blanco et al., 2016). Neutron spectrum unfolding method based on ANNs without normalization can work only if the fluence of neutron field to measure is an unit fluence, which is not the common case in practice. And an unfolded normalized spectrum generally leads to the true values of neutron fluence and  $H^*(10)$  never to be known. To solve this, three normalization methods—zero-mean normalization method, min-max normalization method, and maximum-divided normalization method were introduced to the network inputs, and a new method was proposed for neutron fluence and  $H^*(10)$  estimations derived from unfolded normalized neutron spectrum based on GRNNs.

The aim of this work was to use a four-fold cross validation method to randomly select sixty-three from two hundred fifty-one spectra as the network test data for evaluating and comparing the performance of neutron spectrum unfolding, and estimations of neutron fluence and  $H^*(10)$ , based on GRNNs with three normalization methods for the first time. And experimental measurements were done by BSS in well characterized  $^{241}\text{Am}$ -Be neutron field.

## 2. Materials and methods

Neutron spectrum is physically a continuous function to describe neutron fluence with respect to neutron energy. To derive the neutron spectrum, the discrete form of the homogeneous Fredholm integral equation of the first kind (Wang et al., 2019) is commonly used and is shown in Eq. (1)

$$M_j = \sum_{i=1}^n R_{ij} \phi_i, \quad j = 1, 2, \dots, m, \quad (1)$$

where  $M_j$  is the measured reading by the  $j$ -th Bonner sphere,  $R_{ij}$  is the response of the  $j$ -th sphere at the  $i$ -th energy bin, and  $\phi_i$  is the neutron fluence of the  $i$ -th energy bin. The number of energy bins,  $n$ , is larger than the amount of spheres,  $m$ , therefore Eq. (1) is an ill-conditioned system having an infinite number of spectrum solutions  $\phi$ . The aim of unfolding is to derive the only spectrum as close as possible to the actual one.

In our laboratory, the homemade BSS comprises eight high density polyethylene spheres with 3, 4, 5, 6, 7, 8, 10, and 12 inch diameters, and a single SP9 spherical thermal neutron proportional counter with  $^3\text{He}$  at 304 cm Hg of pressure, which is shared in center of the spheres. The eight responses of BSS to monoenergetic neutrons from  $10^{-9}$  to 400 MeV divided to sixty energy bins were calculated with use of Monte Carlo code MCNP-4B (Briesmeister, 1997). The estimated responses are shown in Fig. 1. The response functions were read by the computational codes for neutron spectrum unfolding based on GRNNs developed in the

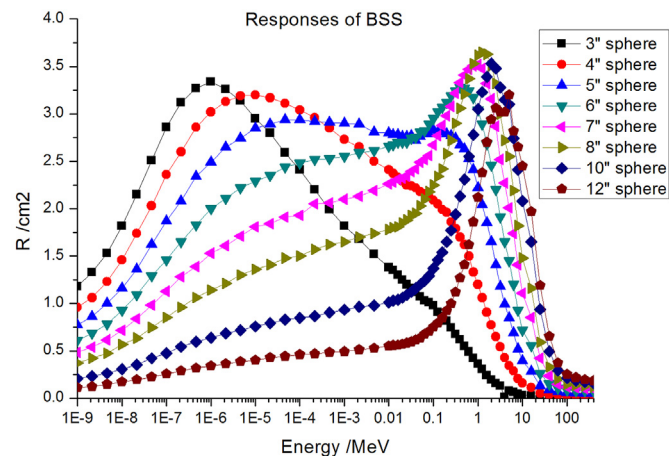


Fig. 1. Responses of Bonner sphere spectrometry (BSS).

MATLAB programming environment (MATLAB and Statistics Toolbox Release, 2009a).

### 2.1. Normalization of inputs for GRNNs

The inputs and the outputs for training the GRNNs were obtained from IAEA (2001). Here, the neutron spectra are per unit of lethargy and were converted to per unit of energy (becoming the outputs). Each spectrum was multiplied by the response matrix (Fig. 1) obtaining the respective counts of each sphere (becoming the inputs). However, the measured sphere readings, generally outside the range of the inputs for training, can not output a neutron spectrum. Thus, the inputs for training and the new input from BSS measurements need to be normalized. Here are three normalization methods:

- Zero-mean normalization method. The method is to form all the inputs to unit variances and zero means. For each set of the input, the mean value  $\mu$  and the standard deviation  $\sigma$  of eight sphere readings are calculated automatically, the eight sphere readings  $M$  substrate the mean value  $\mu$  and divide by the standard deviation  $\sigma$  to form new eight sphere readings  $M^{zm}$  as the normalized input.

$$M_j^{zm} = \frac{M_j - \mu}{\sigma}, \quad j = 1, 2, \dots, 8. \quad (2)$$

- Min-max normalization method. The method is to form all the inputs to the range of 0–1. For each set of the input, the maximum  $M_{max}$  and the minimum  $M_{min}$  of the eight sphere readings are automatically found at first, the eight sphere readings  $M$  substrate the minimum  $M_{min}$  and divide by the difference between the maximum  $M_{max}$  and the minimum  $M_{min}$  to form new eight sphere readings  $M^{mm}$  as the normalized input.

$$M_j^{mm} = \frac{M_j - M_{min}}{M_{max} - M_{min}}, \quad j = 1, 2, \dots, 8. \quad (3)$$

- Maximum-divided normalization method. The method is to form all the inputs smaller or equal to 1. For each set of the input, the maximum  $M_{max}$  of eight sphere readings are automatically found at first, the eight sphere readings  $M$  divide by the maximum  $M_{max}$  to form new eight sphere readings  $M^{md}$  as the normalized input.

$$M_j^{md} = \frac{M_j}{M_{max}}, \quad j = 1, 2, \dots, 8. \quad (4)$$

### 2.2. Optimization of spread constant

Spread constant, as the only parameter to be optimized has great

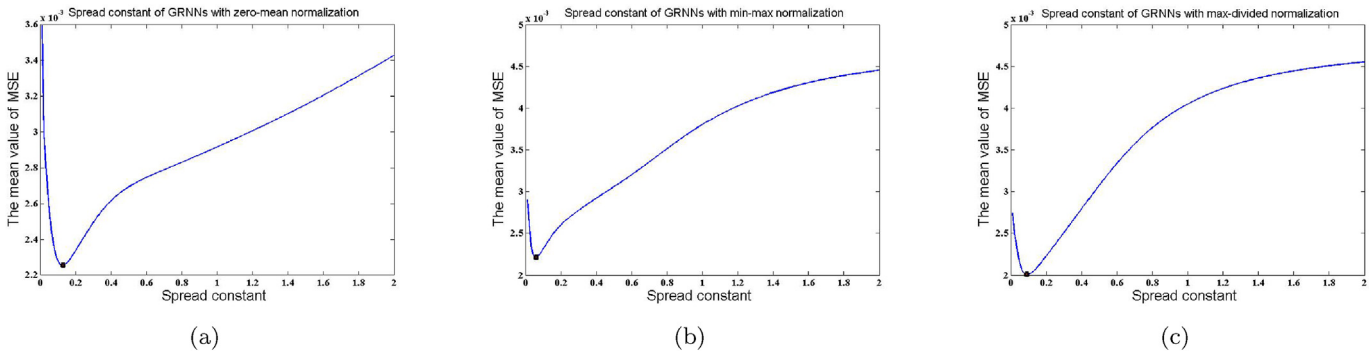


**Fig. 2.** The mean values of mean squared errors (MSEs) corresponds to spread constants in the range from 0.01 to 2 in increments of 0.01 for GRNNs based on three normalization methods. (a) The marked optimum spread constant is 0.13 for GRNNs based on zero-mean normalization method. (b) The marked optimum spread constant is 0.06 for GRNNs based on min-max normalization method. (c) The marked optimum spread constant is 0.09 for GRNN based on maximum-divided normalization method. GRNNs, generalized regression neural networks.

impact on generalization capabilities of GRNNs. In general, larger spread constant leads to a smoother Gaussian radial basis function (RBF) and thus a more similar manner of all the neurons to the inputs, smaller spread constant leads to the input space more difficult to be thoroughly covered. Spread constant optimization from 200 values varying from 0 to 2 in increments of 0.01 was realized through the leave-one-out cross validation technique. Each spectrum out of two hundred fifty-one from IAEA (2001) was chosen as the testing spectrum in turn, while the remaining spectra played the roles as training data, the mean value of 251 mean squared errors (MSEs) between unfolded normalized spectra  $\phi^{un}$  and actual normalized spectra  $\phi^{an}$  defined by Eq. (5) was used for network performance evaluation and plotted in Fig. 2. 50,200 neural networks (i.e., 200 spread constants  $\times$  251 spectra) were created for GRNNs based on each normalization method. The optimum spread constant is 0.13 for GRNNs based on zero-mean normalization method, 0.06 for GRNNs based on min-max normalization method, and 0.09 for GRNNs based on maximum-divided normalization method.

$$\text{MSE} = \frac{1}{60} \sum_{i=1}^{60} [\phi_i^{un} - \phi_i^{an}]^2. \quad (5)$$

### 2.3. Neutron fluence and $H^*(10)$ estimation technique

Generally, total neutron fluence  $\Phi$  can be obtained by integrating the neutron spectrum  $\phi$  over neutron energy, as shown in Eq. (6). However, the outputs for training the GRNNs are normalized spectra extracted from IAEA (2001). Thus, GRNNs outputs a normalized unfolded spectrum when a new input is given, which leads to  $\Phi = 1\text{cm}^{-2}$  a priori.

To obtain the true value of total neutron fluence  $\Phi$ , one thought is to break the spectrum normalization structure for training GRNNs by multiplying random fluence values, but this makes the data for training GRNNs extremely huge and the performance of neutron spectrum unfolding not worth expecting. Here, a new method is introduced on the basis of the unfolded normalized spectra from GRNNs for total neutron fluence estimation.

Unfolded sphere readings  $M^{un}$  can be obtained from the unfolded normalized spectra  $\phi^{un}$  and the response matrix  $R$ , shown in Eq. (7). Here, the value of total neutron fluence  $\Phi_g$  can be regarded as the mean ratio of the measured sphere readings  $M$  and unfolded sphere readings  $M^{un}$ , shown in Eq. (8).

The true unfolded spectrum  $\phi^{tu}$  is the unfolded normalized spectra  $\phi^{un}$  multiplied by the value of total neutron fluence  $\Phi_g$ , shown in Eq. (9). And the true calculated sphere readings  $M^{cal}$  are unfolded sphere readings  $M^{un}$  multiplied by the value of total neutron fluence  $\Phi_g$ , shown in Eq. (10). The corresponding  $H^*(10)$  can be obtained using the true

unfolded spectrum  $\phi^{tu}$  and the fluence-to-ambient dose equivalent conversion coefficients  $h_\phi$  from ICRP Publication 74 (1996), shown in Eq. (11).

$$\Phi = \sum_{i=1}^n \phi_i. \quad (6)$$

$$M_j^{un} = \sum_{i=1}^{60} R_{ij} \phi_i^{un} \quad j = 1, 2, \dots, 8, \quad (7)$$

$$\Phi_g = \frac{1}{8} \sum_{j=1}^8 \frac{M_j}{M_j^{un}}, \quad (8)$$

$$\phi_i^{tu} = \Phi_g \phi_i^{un}, \quad i = 1, 2, \dots, 60. \quad (9)$$

$$M_i^{cal} = \Phi_g M_i^{un}, \quad j = 1, 2, \dots, 8. \quad (10)$$

$$H_{cal}^*(10) = \sum_{i=1}^{60} \phi_i^{tu} h_{\phi,i} \quad (11)$$

## 2.4. Testing results and discussions

In order to assess the performance of neutron spectrum unfolding and estimations of neutron fluence and  $H^*(10)$  based on GRNNs with three normalization methods, a four-fold cross validation method were used. One fourth of 251 neutron spectra (i.e., 63 spectra) were randomly chosen, they were respectively multiplied by given pseudo-random fluence values as the expected test spectra, while the remaining spectra without any treatment played the roles as the training data.

The spectral quality  $Q_s$  in Eq. (12) and the sphere reading quality  $Q_r$  in Eq. (13) were used for unfolding performance assessment. A perfect unfolded neutron spectrum leads to  $Q_s$  and  $Q_r$  equal to zero.  $Q_\Phi$  and  $Q_d$  are respectively defined in Eq. (14) and Eq. (15) for neutron fluence and  $H^*(10)$  assessment, and perfect estimations lead to  $Q_\Phi$  and  $Q_d$  equal to zero.

$$Q_s = \left[ \frac{\sum_{i=1}^{60} [\phi_i^{tu} - \phi_i]^2}{\sum_{i=1}^{60} \phi_i^2} \right]^{1/2}, \quad (12)$$

$$Q_r = \left[ \frac{1}{8} \sum_{j=1}^8 \left( \frac{M_j^{cal} - M_j}{M_j} \right)^2 \right]^{1/2}. \quad (13)$$

$$Q_\Phi = \frac{|\Phi_g - \Phi|}{\Phi} \quad (14)$$

$$Q_d = \frac{|H_{cal}^*(10) - H^*(10)|}{H^*(10)} \quad (15)$$

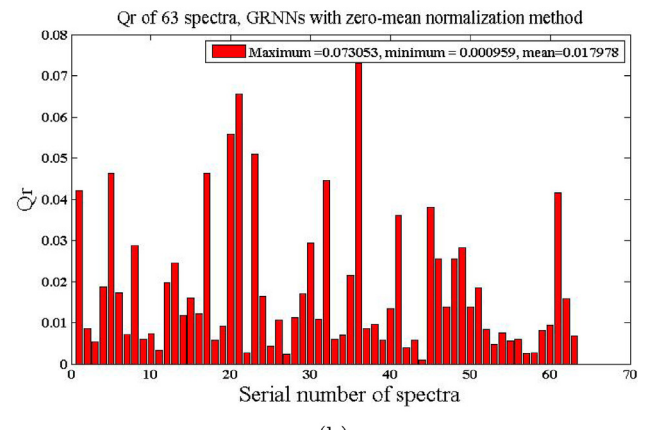
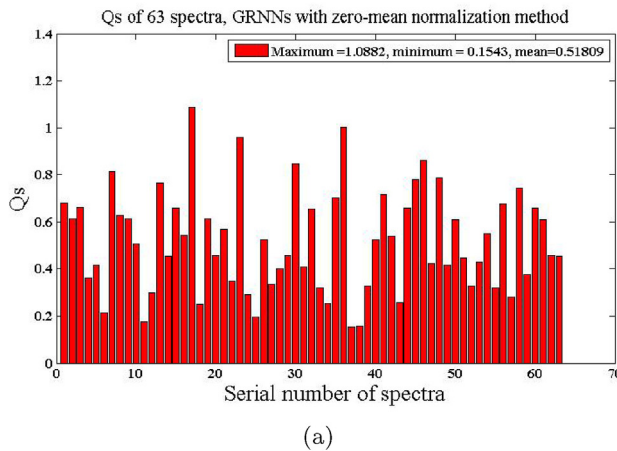


**Fig. 3.**  $Q_s$  and  $Q_r$  of 63 neutron spectra obtained by the generalized regression neural networks (GRNNs) with use of zero-mean normalization method for evaluating unfolding performance. (a) For  $Q_s$ , the maximum is 1.0882, the minimum is 0.1543, and the mean is 0.51809. (b) For  $Q_r$ , the maximum is 0.073053, the minimum is 0.000959, and the mean is 0.017978.

#### 2.4.1. Testing results of zero-mean normalization method

The testing results based on GRNNs with zero-mean normalization method were shown below:

- For assessment of unfolding performance,  $Q_s$  and  $Q_r$  of 63 testing neutron spectra were plotted.  $Q_s$  were shown in Fig. 3(a) with the maximum of 1.0882, the minimum of 0.1543, and the mean of 0.51809.  $Q_r$  were plotted in Fig. 3(b) with the maximum of 0.073053, the minimum of 0.000959, and the mean of 0.017978.
- Total neutron fluences by calculation  $\Phi_g$  and pseudo-random expected neutron fluences  $\Phi$  were plotted in Fig. 4(a).  $Q_\Phi$  were calculated and shown in Fig. 4(b) with the maximum of 42.62%, the minimum of 0.15054%, and the mean of 8.7113%.
- Calculated  $H_{cal}^*(10)$  and the corresponding expected  $H^*(10)$  were plotted in (a).  $Q_d$  were shown in Fig. 5(b) with the maximum of 101.6667%, the minimum of 0.15735%, and the mean of 23.774%.

#### 2.4.2. Testing results of min-max normalization method

The testing results based on GRNNs with min-max normalization method were shown below:

- $Q_s$  were shown in Fig. 6(a) with the maximum of 0.96866, the

minimum of 0.18198, and the mean of 0.50764.  $Q_r$  were plotted in Fig. 6(b) with the maximum of 0.077449, the minimum of 0.001110, and the mean of 0.021326.

- Total neutron fluences by calculation  $\Phi_g$  and the corresponding expected neutron fluences  $\Phi$  were plotted in Fig. 7(a).  $Q_\Phi$  were calculated and shown in Fig. 7(b) with the maximum of 35.9066%, the minimum of 0.02889%, and the mean of 8.7138%.
- Calculated  $H_{cal}^*(10)$  and the corresponding expected  $H^*(10)$  were plotted in Fig. 8(a).  $Q_d$  were shown in Fig. 8(b) with the maximum of 139.0566%, the minimum of 0.48244%, and the mean of 27.1212%.

#### 2.4.3. Testing results of maximum-divided normalization method

The testing results based on GRNNs with maximum-divided normalization method were shown below:

- $Q_s$  were shown in Fig. 9(a), with the maximum of 0.90789, the minimum of 0.18036, and the mean of 0.44693.  $Q_r$  were plotted in Fig. 9(b), with the maximum of 0.037038, the minimum of 0.002042, and the mean of 0.008651.
- Total neutron fluences by calculation  $\Phi_g$  and the corresponding expected neutron fluences  $\Phi$  were plotted in Fig. 10(a).  $Q_\Phi$  were calculated and shown in Fig. 10(b) with the maximum of 29.5492%, the minimum of 0.0224%, and the mean of 6.9109%.
- Calculated  $H_{cal}^*(10)$  and the corresponding expected  $H^*(10)$  were

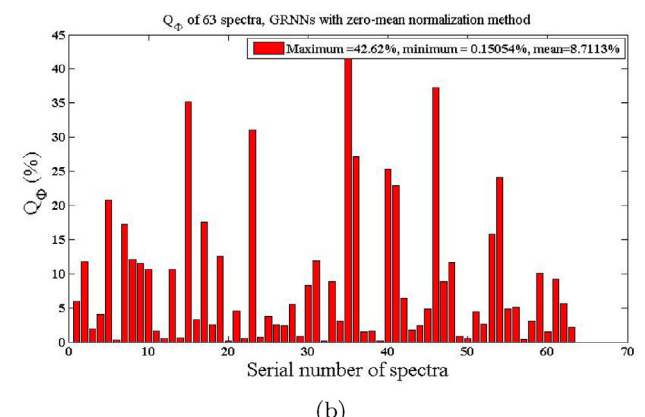
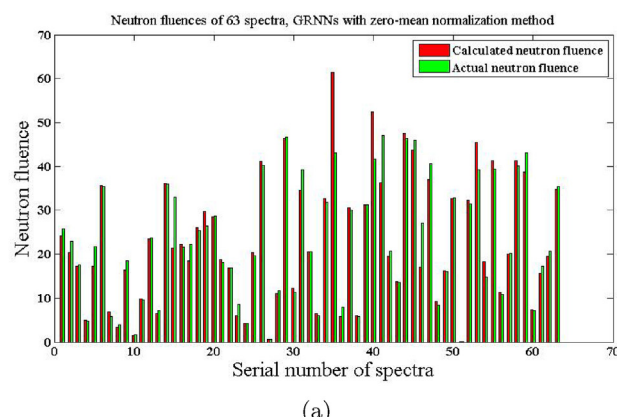


**Fig. 4.** Total neutron fluence  $\Phi$  and  $Q_\Phi$  of 63 neutron spectra obtained by the generalized regression neural networks (GRNNs) with use of zero-mean normalization method. (a) The left bar of each set corresponds to the total neutron fluence  $\Phi_g$  by calculation, and the right bar of each set corresponds to the actual neutron fluence  $\Phi$ . (b) For  $Q_\Phi$ , the maximum is 42.62%, the minimum is 0.15054%, and the mean is 8.7113%.

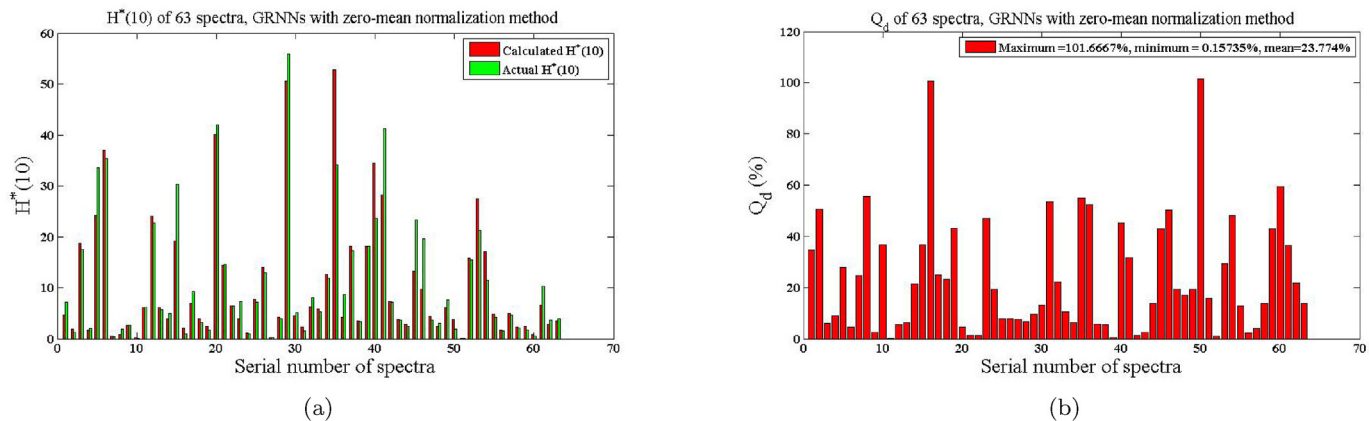


**Fig. 5.**  $H^*(10)$  and  $Q_d$  of 63 neutron spectra obtained by the generalized regression neural networks (GRNNs) with use of zero-mean normalization method. (a) The left bar of each set corresponds to the  $H_{\text{cal}}^*(10)$  by calculation, and the right bar of each set corresponds to the actual  $H^*(10)$ . (b) For  $Q_d$ , the maximum is 101.6667%, the minimum is 0.15735%, and the mean is 23.774%.

plotted in Fig. 11(a).  $Q_d$  were shown in Fig. 11(b) with the maximum of 116.7371%, the minimum of 0.2484%, and the mean of 17.9242%.

#### 2.4.4. Comparisons and discussions

The performance of neutron spectrum unfolding based on GRNNs with three normalization methods was evaluated by comparing the mean spectral quality  $Q_s$  and the mean sphere reading quality  $Q_r$ , while the assessments of neutron fluence and  $H^*(10)$  were respectively by the mean  $Q_\Phi$  and the mean  $Q_d$ . GRNN with use of maximum-divided method is the best method though the comparisons of quality parameters shown in Table 1. The generalization capabilities of neutron fluence and  $H^*(10)$  estimations are acceptable with the mean  $Q_\Phi$  within 7% and the mean  $Q_d$  within 18%. Furthermore, the mean  $Q_s$  and the mean  $Q_r$  of the same 63 testing spectra based on GRNNs with maximum-divided normalization method, GRNN without normalization method, and genetic algorithm (GA) method were compared in Table 2. For the mean spectral quality  $Q_s$ , the indispensable normalization process to the inputs for practical use decreases the accuracy of GRNNs, but still better than GA method. And the mean sphere reading quality  $Q_r$  has greatly improved by introducing the new neutron fluence estimation method.

### 3. Experiment and discussions

In order to evaluate the performance of GRNNs, using the

maximum-divided normalization method, to unfold the neutron spectrum and to calculate the neutron fluence and  $H^*(10)$ , the BSS with the  ${}^3\text{He}$  proportional counter was used to measure a  ${}^{241}\text{Am}$ -Be neutron source. Measurements were carried out at the Department of Radiation Protection and Monitoring in Wuhan Second Ship Design and Research Institute. The signal processing system of the BSS includes a pre-amplifier and a local processing and displaying unit (LPDU) which assembles high-voltage module, power supply, signal processing board and displaying board in a box. An appropriate discrimination level was set in the signal processing board to reject the signals from photons and electric noises (Le et al., 2018). And a shadow cone technique was used to eliminate the effects from room-scattered neutron events (Yamaguchi et al., 1999).

The  ${}^{241}\text{Am}$ -Be neutron source strength  $S$  is  $9.65 \times 10^6 \pm 1.1\% \text{ s}^{-1}$ , and the distance  $d$  between the center of Bonner sphere and the center of point-like neutron source is  $200 \pm 0.5\% \text{ cm}$  in the experiment. Using Eq. (16), the theoretical total neutron fluence rate is  $19.2 \pm 2.1\% \text{ cm}^{-2}\text{s}^{-1}$ . Using Eq. (17), the  $H_{\text{the}}^*(10)$  rate is  $27.03 \pm 2.1\% \mu\text{Sv}/\text{h}$ , where  $h_\varphi$  is fluence-to-ambient dose equivalent conversion coefficient for  ${}^{241}\text{Am}$ -Be of 391  $\text{pSv} \cdot \text{cm}^2$  (ISO, 2001).

$$\dot{\Phi}_{\text{the}} = \frac{S}{4\pi d^2} \quad (16)$$

$$\dot{H}_{\text{the}}^*(10) = \dot{\Phi}_{\text{the}} \times h_\varphi \quad (17)$$

The measured count rates for each of the Bonner spheres, with the shadow cone, without the shadow cone, and the difference were listed

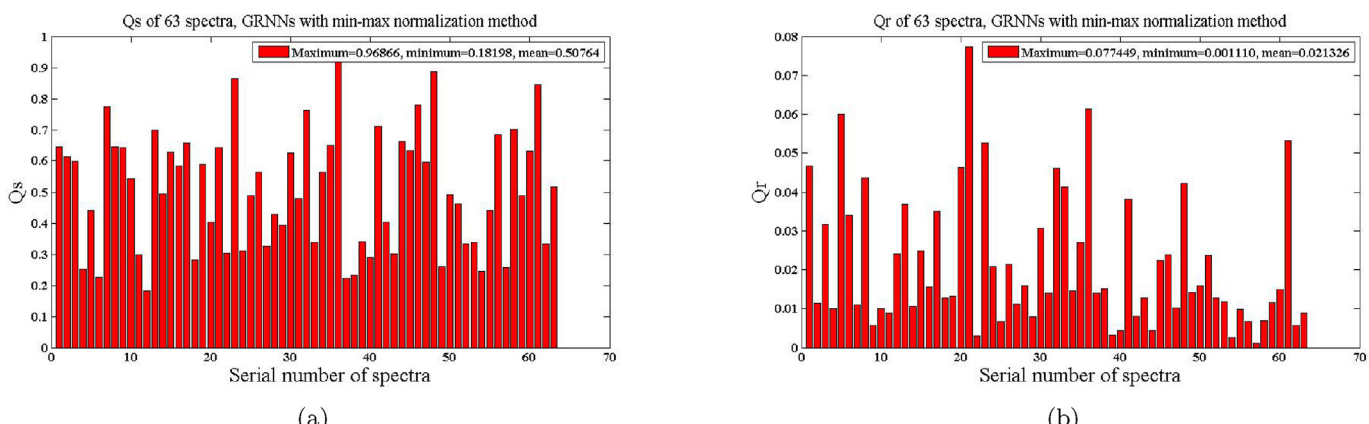
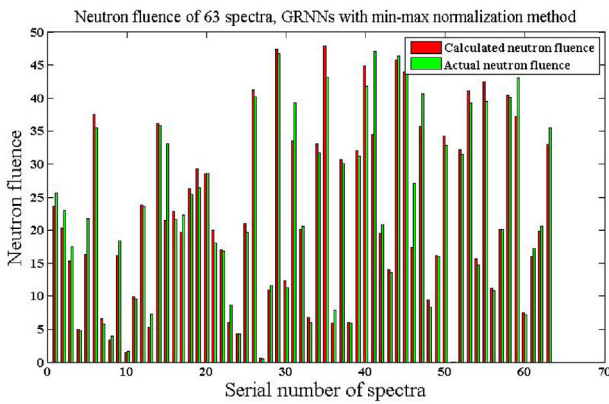
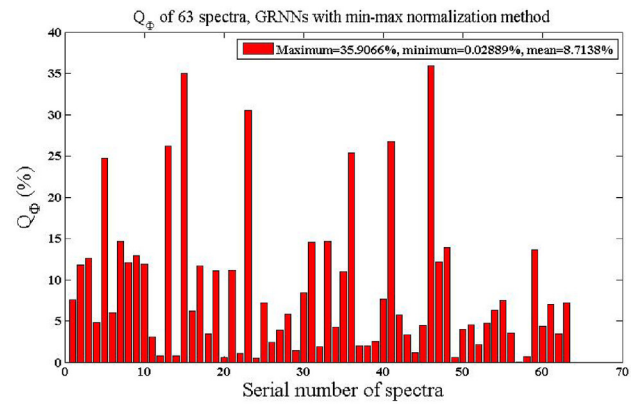


**Fig. 6.**  $Q_s$  and  $Q_r$  of 63 neutron spectra obtained by the generalized regression neural networks (GRNNs) with use of min-max normalization method for evaluating unfolding performance. (a) For  $Q_s$ , the maximum is 0.96866, the minimum is 0.18198, and the mean is 0.50764. (b) For  $Q_r$ , the maximum is 0.077449, the minimum is 0.001110, and the mean is 0.021326.



(a)



(b)

**Fig. 7.** Total neutron fluence  $\Phi$  and  $Q_\Phi$  of 63 neutron spectra obtained by the generalized regression neural networks (GRNNs) with use of min-max normalization method. (a) The left bar of each set corresponds to the neutron fluence  $\Phi_g$  by calculation, and the right bar of each set corresponds to the actual neutron fluence  $\Phi$ . (b) For  $Q_\Phi$ , the maximum is 35.9066%, the minimum is 0.02889%, and the mean is 8.7138%.

in Table 3.

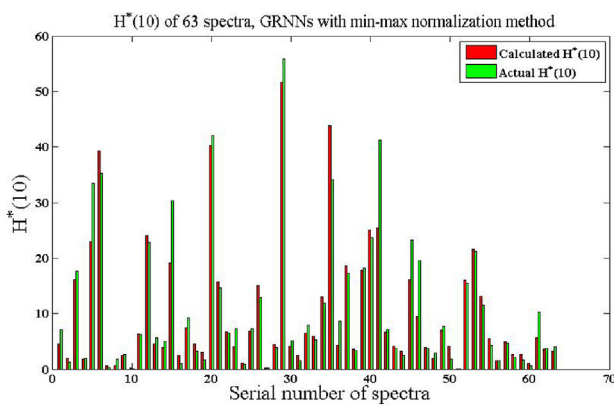
The BSS calibration factor,  $F$ , as the mean value of eight ratios between the net count rates by measurements and by MCNP-4B simulation per unit fluence, is 0.508 and shown in Fig. 12.  $F$  is lower than 1 because not all the neutron reaction events in neutron counter can produce measurable signals (Bedogni et al., 2015). Moreover, The ratio between the count rates by measurements and by simulations decreases as the diameter of Bonner sphere increases. The reason is that the shadow cones used for larger Bonner spheres are not big enough to fully shield the direct neutron irradiation leading to the lower net count rates, and too large for smaller Bonner spheres leading to the higher net count rates.

The unfolded  $^{241}\text{Am}$ -Be neutron spectra based on GRNNs with use of maximum-divided normalization method derived from the measured count rates and the simulated count rates, and based on MAXED method (Reginatto et al., 2002) with initial guess from Alegra et al. (1992), with the measured count rates and the simulated count rates were shown in Fig. 13. And the corresponding calculated count rates were plotted in Fig. 14.

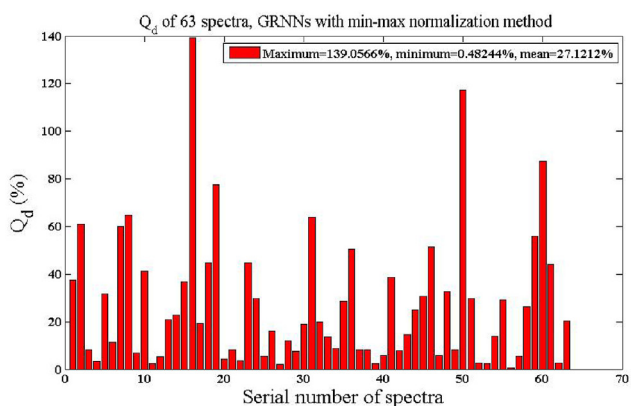
GRNNs with maximum-divided normalization method without the need of an initial guess is mainly dependent on the count rates. Compared with the unfolded spectrum using GRNN with simulated count rates, the unfolded spectrum using GRNN with measured count rates shows obviously thermal and epithermal neutrons, this is due to

the higher net count rates by measurements for smaller Bonner spheres, especially for 3 and 4 inch spheres (Fig. 12). And the lower count rates by measurements for larger Bonner spheres, especially for 10 and 12 inch spheres (Fig. 12), leading to a smaller peak with narrow width in the large energy region. While, MAXED method is strongly dependent on the initial guess for neutron spectrum unfolding, and the count rates are used to adjust the local optimum. Compared with the unfolded spectrum using MAXED method with simulated count rates, the unfolded spectrum using MAXED method with measured count rates shows a slightly higher curve in thermal and epithermal region, and a lower peak with narrow width. The reason is also higher count rates for small Bonner spheres and lower count rates for larger Bonner spheres.

The neutron fluence rates,  $H^*(10)$  rates,  $Q_\Phi$  and  $Q_d$  calculated by different methods were listed in Table 4. From the results, MAXED method showed better agreements with the theoretical values than GRNNs with maximum-divided normalization method for neutron fluence rate and  $H^*(10)$  rate estimations. When the count rates by BSS measurements were used, MAXED method gave  $Q_\Phi$  of 8.02% and  $Q_d$  of 5.73%, while GRNNs with maximum-divided normalization method gave acceptable but relatively large  $Q_\Phi$  of 17.8% and  $Q_d$  of 17.2%. However, when the count rates simulated by MCNP-4B were used, both method showed great neutron fluence rate and  $H^*(10)$  rate estimation ability. MAXED method gave  $Q_\Phi$  of 0.26% and  $Q_d$  of 0.63% which are both less than the calculation uncertainties 2.1%. While GRNNs with

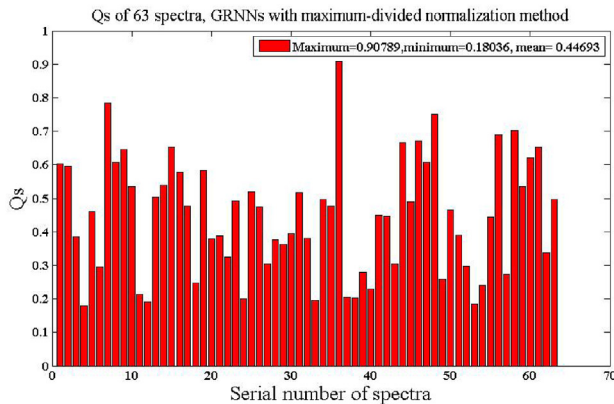


(a)

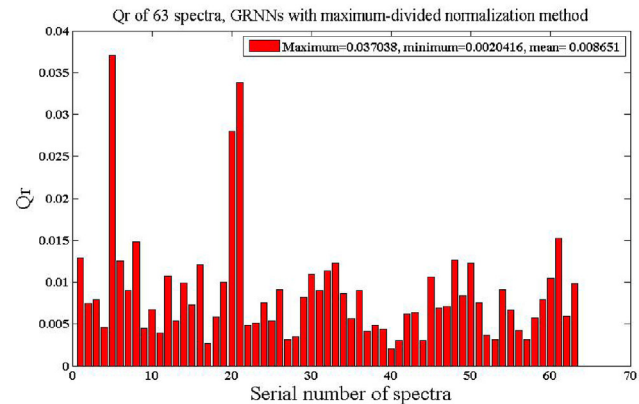


(b)

**Fig. 8.**  $H^*(10)$  and  $Q_d$  of 63 neutron spectra obtained by the generalized regression neural networks (GRNNs) with use of min-max normalization method. (a) The left bar of each set corresponds to the  $H_{cal}^*(10)$  by calculation, and the right bar of each set corresponds to the actual  $H^*(10)$ . (b) For  $Q_d$ , the maximum is 139.0566%, the minimum is 0.48244%, and the mean is 27.1212%.

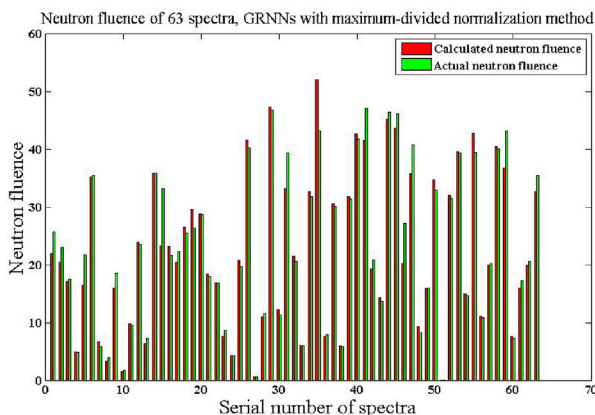


(a)

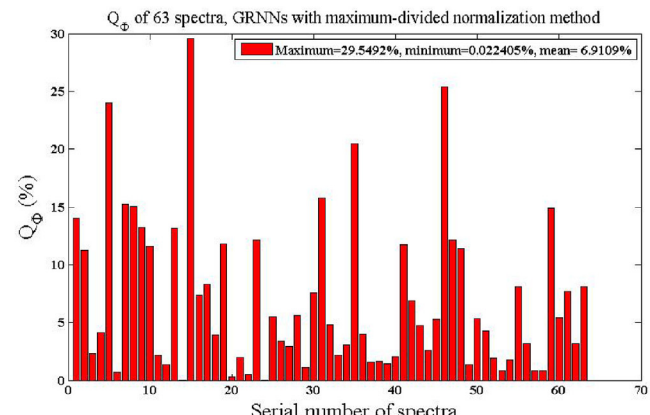


(b)

**Fig. 9.** Q<sub>s</sub> and Q<sub>r</sub> of 63 neutron spectra obtained by the generalized regression neural networks (GRNNs) with use of maximum-divided normalization method for evaluating unfolding performance. (a) For Q<sub>s</sub>, the maximum is 0.90789, the minimum is 0.18036, and the mean is 0.44693. (b) For Q<sub>r</sub>, the maximum is 0.037038, the minimum is 0.002042, and the mean is 0.008651.

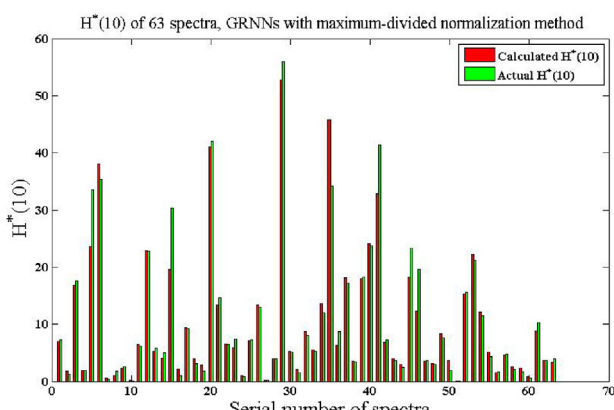


(a)

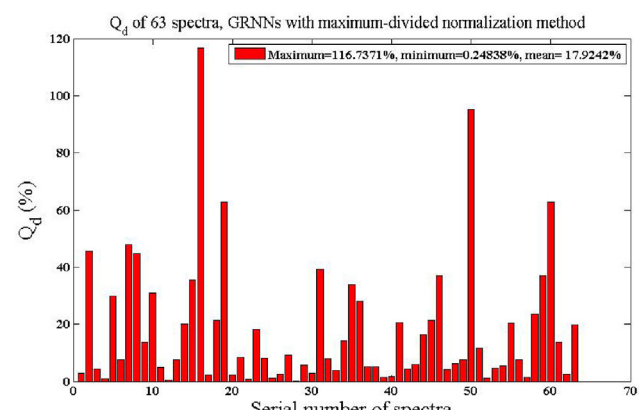


(b)

**Fig. 10.** Total neutron fluence  $\Phi$  and  $Q_\Phi$  of 63 neutron spectra obtained by the generalized regression neural networks (GRNNs) with use of maximum-divided normalization method. (a) The left bar of each set corresponds to the neutron fluence  $\Phi_g$  by calculation, and the right bar of each set corresponds to the actual neutron fluence  $\Phi$ . (b) For  $Q_\Phi$ , the maximum is 29.5492%, the minimum is 0.0224%, and the mean is 6.9109%.



(a)



(b)

**Fig. 11.** H\*(10) and Q<sub>d</sub> of 63 neutron spectra obtained by the generalized regression neural networks (GRNNs) with use of maximum-divided normalization method. (a) The left bar of each set corresponds to the  $H_{cal}^*(10)$  by calculation, and the right bar of each set corresponds to the actual  $H^*(10)$ . (b) For  $Q_d$ , the maximum is 116.7371%, the minimum is 0.2484%, and the mean is 17.9242%.

**Table 1**

Quality parameters of generalized regression neural networks (GRNNs) with use of three normalization methods.

Normalization method	Mean $Q_s$	Mean $Q_r$	Mean $Q_\Phi$	Mean $Q_d$
Zero-mean	0.51809	0.017978	8.7113	23.774
Min-max	0.50764	0.021326	8.7138	27.1212
Maximum-divided	0.44693	0.00861	6.9109	17.9242

**Table 2**

Quality parameters of three methods for assessment of neutron spectrum unfolding performance.

Neutron spectrum unfolding method	Mean $Q_s$	Mean $Q_r$
GRNNs with Maximum-divided normalization method	0.44693	0.00861
GRNNs without normalization method	0.3685	0.1695
Genetic algorithm method	0.5175	0.0620

**Table 3**

Measured count rates of the Bonner spheres.

Size (inch)	Without the shadow cone (cps)	With the shadow cone (cps)	The difference (cps)
3	9.63	7.63	2
4	18	11	7
5	26.3	12.8	13.5
6	31.9	13.5	18.4
7	34.2	12.7	21.5
8	35.3	11.5	23.8
10	32.7	8	24.7
12	26.2	5.38	20.82

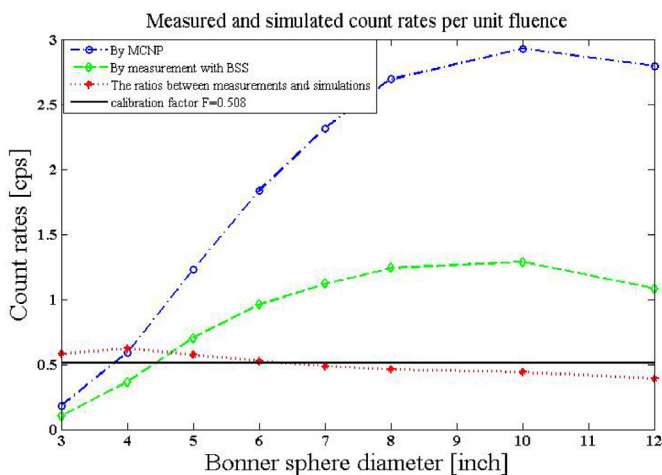


**Fig. 12.** The count rates by measurement and by MCNP-4B simulation of eight spheres per unit fluence are respectively linked by green rhombuses and blue circles. The ratios are marked red dots, and the calibration factor equals to 0.508 which is a black horizontal line. (For interpretation of the references to colour in this figure legend, the reader is referred to the Web version of this article.)

maximum-divided normalization method gave  $Q_\Phi$  of 2.86% very close to the calculation uncertainty and  $Q_d$  0.63% within the calculation uncertainty. MAXED unfolding method is superior, while GRNN with maximum-divided normalization method without the need of an initial guess can be more widely used in practice.

#### 4. Conclusions

GRNN method, as a good candidate to unfold neutron spectrum without the initial guess, cannot be used in practice without the

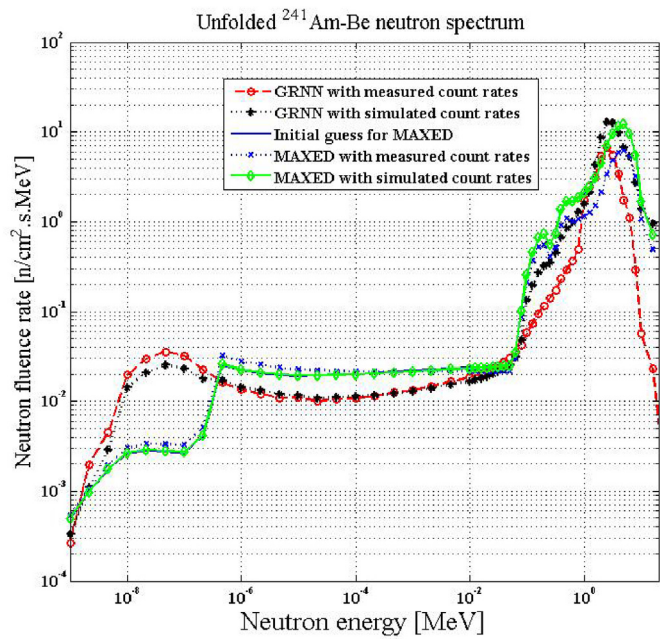


**Fig. 13.** Unfolded  $^{241}\text{Am-Be}$  neutron spectra based on GRNNs with use of maximum-divided normalization method derived from the measured count rates and simulated count rates are respectively linked by red circles and black stars. The initial guess spectrum for MAXED method is linked by blue line. And the unfolded spectra based on MAXED method with measured count rates and simulated count rates are respectively linked by blue crosses and green rhombuses. (For interpretation of the references to colour in this figure legend, the reader is referred to the Web version of this article.)

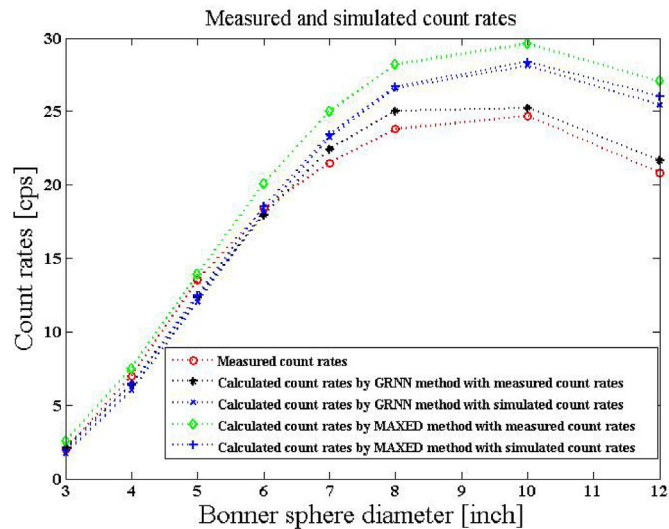


**Fig. 14.** The count rates by measurement are linked by red circles, and the count rates calculated by GRNNs with use of maximum-divided normalization method derived from the measured and simulated count rates are respectively linked by black stars and blue crosses, and the count rates calculated by MAXED method with measured and simulated count rates are respectively linked by green rhombuses and blue plus signs. (For interpretation of the references to colour in this figure legend, the reader is referred to the Web version of this article.)

normalization method, and cannot directly give neutron fluence and  $H^*(10)$ . In this work, the issues have been solved by using three normalization methods to the inputs of GRNNs and a new method to derive the neutron fluence and  $H^*(10)$  from the unfolded normalized spectrum.

**Table 4**Neutron fluence rate and  $H^*(10)$  rate estimations.

	Neutron fluence rate ( $n/cm^2 \cdot s$ )	$H^*(10)$ rate ( $\mu\text{Sv}/\text{h}$ )	$Q_\Phi$	$Q_d$
True value	19.2	27.03	0	0
GRNNs with BSS measurements	15.78	22.37	17.8%	17.2%
GRNNs with MCNP-4B simulations	18.65	27.20	2.86 %	0.63 %
MAXED with BSS measurements	20.74	28.58	8.02 %	5.73%
MAXED with MCNP-4B simulations	19.25	27.20	0.26 %	0.63%

Sixty-three neutron spectra were unfolded based on GRNNs with use of the three normalization methods for neutron fluence and  $H^*(10)$  estimations, the testing results showed that the maximum-divided normalization method is the best with the mean  $Q_\Phi$  within 7% and the mean  $Q_d$  within 18% which are acceptable in practical use, especially for unknown neutron field measurements.

The experimental measurement by BSS in well characterized  $^{241}\text{Am}$ -Be neutron field had been done. GRNNs with the maximum-divided normalization method and MAXED method were used to unfold the neutron spectrum and to calculate neutron fluence rate and  $H^*(10)$  rate. The relatively large values of quality parameters  $Q_\Phi$  and  $Q_d$  were mainly due to the shadow cones, but were still acceptable. More experiments in monoenergy neutron field and other well characterized neutron field (i.e., such as  $^{252}\text{Cf}$  neutron field) are needed for improving the accuracy of calibration factor. However, with use of the count rates by MCNP-4B simulations, the neutron fluence rate and  $H^*(10)$  rate by two methods agreed well with the theoretical values.

GRNN method relies on the amount and the diversity of training spectra data for neutron spectrum unfolding. And a different GRNN must be trained and tested for a different set of response functions. Compared with MAXED method, GRNN method do not show better performance. However, GRNN method do not need an initial guess spectrum and can be more widely used in practice. It is a proven high performance neutron spectrum unfolding candidate for neutron fluence and  $H^*(10)$  estimations.

## References

- Alevra, A., Klein, H., Knauf, K., Wittstock, J., 1992. Neutron field spectrometry for radiation protection dosimetry purposes. *Radiat. Prot. Dosim.* 44, 223–226.
- Andersson, L., Braun, J., 1963. A neutron Rem counter with uniform sensitivity from 0.025eV to 10 MeV. *Proc. IAEA Symp. On Neutron Dosim.*, Vienna, vol. 2. pp. 87–95.
- Arbib, M., 2003. Brain Theory and Neural Networks. The MIT Press.
- Bartlett, D., Tanner, R., Jones, D., 1997. A new design of neutron dose equivalent survey instrument. *Radiat. Prot. Dosim.* 74 (1–2), 267–271.
- Bedogni, R., Gomez-Ros, J., Pola, A., Bortot, D., Gentile, A., Introini, M., Buonomo, B., Lorenzoli, M., Mazzitelli, M., Sacco, D., 2015. Experimental test of a newly developed single-moderator, multi-detector, directional neutron spectrometer in reference monochromatic fields from 144KeV to 16.5MeV. *Nucl. Instrum. Methods phys. Res. Sect. A* 782, 35–39.
- Bing, C., Titterington, D., 1994. Neural networks: a review from a statistical perspective. *Stat. Sci.* 9 (1), 2–30.
- Birattari, C., Ferrari, A., Nuccetelli, C., Pelliccioni, M., Silari, M., 1990. An extended range neutron rem counter. *Nucl. Instrum. Methods* 297 (1–2), 250–257.
- Braga, C., Dias, M., 2002. Application of neural networks for unfolding neutron spectra measured by means of Bonner spheres. *Nucl. Instrum. Methods Phys. Res., Sect. A* 476 (1–2), 252–255.
- Bramblett, R., Ewing, R., Bonner, T., 1960. A new type of neutron spectrometer. *Nucl. Instrum. Methods* 9 (1), 1–12.
- Briesmeister, J., 1997. MCNP™-A General Monte Carlo N-Particle Transport Code. Version 4B. Los Alamos National Laboratory Report LA12625-M.
- Fehrenbacher, G., Schutz, R., Hahn, K., Sprunck, M., Cordes, E., Biersack, J., Wahl, W., 1999. Proposal of a new method for neutron dosimetry based on information obtained by application of artificial neural networks. *Radiat. Prot. Dosim.* 83, 293–301.
- Guzman-Garcia, K., Mendez-Villafane, R., Vega-Carrillo, H., 2015. Neutron field characteristics of ciemat's neutron standards laboratory. *Appl. Radiat. Isot.* 100, 84–90.
- IAEA, 2001. Compendium of neutron spectra and detector response for radiation protection purpose. Supplement to Technical Reports Series No. 318 IAEA Technical Report Series No. 403.
- ICRP Publication 74, 1996. Conversion coefficients for use in radiological protection against external radiation. Technical report. Ann. ICRP 26, 3–4.
- ISO, 2001. Reference Neutron Radiations Part 1: Characteristics and Methods of Production Technical Report, pp. 32 Switzerland 8529-1:2001(E).
- Kardan, M., Setayeshi, S., Koohi-Fayegh, R., Ghiasi-Nejad, M., 2003. Neutron spectra unfolding in Bonner sphere spectrometry using neural networks. *Radiat. Prot. Dosim.* 104 (1), 27–30.
- Knoll, G., 1999. Radiation Detection and Measurement, third ed. John Wiley & Sons, New York.
- Le, T., Tran, H., Nguyen, Q., Trinh, G., Nguyen, K., 2018. Characterization of a neutron calibration field with  $^{241}\text{Am}$ -Be source using Bonner sphere spectrometer. *Appl. Radiat. Isot.* 133, 68–74.
- Leake, J., 1966. A spherical dose equivalent neutron detector. *Nucl. Instrum. Methods* 45 (1), 151–156.
- Martinez-Blanco, R., Ornelas-Vargas, G., Castaneda-Miranda, C., Solis-Sanchez, L., Castaneda-Miranada, R., Vega-Carrillo, H., Celaya-Padilla, J., Garza-Veloz, I., Martinez-Fierro, M., Ortiz-Rodriguez, J.M., 2016. A neutron spectrum unfolding code based on generalized regression artificial neural networks. *Appl. Radiat. Isot.* 117, 8–14.
- Reginatto, M., Goldhagen, P., Neumann, S., 2002. Spectrum unfolding sensitivity analysis and propagation on uncertainties with the maximum entropy deconvolution code MAXED. *Nucl. Instrum. Methods Phys. Res., Sect. A* 476, 242–246.
- Vega-Carrillo, H., Barquer, R., Mercado, G., 2013. Passive neutron area monitor with CR39. *Int. J. Radiat. Res.* 11 (3), 149–153.
- Vega-Carrillo, H., Guzman-Garcia, K., Gallego, E., Lorente, A., 2014. Passive neutron area monitor with pairs of TLDs as neutron detector. *Radiat. Meas.* 69, 30–34.
- Vega-Carrillo, H., Hernandez-Davila, M., Manzanares-Acuna, E., Mercado, G., Gallego, E., 2005. Artificial neural networks in neutron dosimetry. *Radiat. Prot. Dosim.* 118 (3), 251–259.
- Vega-Carrillo, H., Hernandez-Davila, V., Manzanares-Acuna, E., Gallego, E., Lorente, A., Iniguez, M.P., 2007. Artificial neural networks technology for neutron spectrometry and dosimetry. *Radiat. Prot. Dosim.* 126 (1–4), 408–412.
- Vega-Carrillo, H., Hernandez-Davila, V., Manzanares-Acuna, E., Mercado-Sanchez, G.A., Barquiero, R., Palacios, F., Mendez-Villafane, R., Arteaga-Arteaga, T., Ortiz-Rodriguez, J., 2006. Neutron spectrometry using artificial neural networks. *Radiat. Meas.* 41, 425–431.
- Wang, J., Zhou, Y., Guo, Z., Liu, H., 2019. Neutron spectrum unfolding using three artificial intelligence optimization methods. *Appl. Radiat. Isot.* 147, 136–143.
- Yamaguchi, S., Uritani, A., Sakai, H., Mori, C., Iguchi, T., Toyokawa, H., Takeda, N., Kudo, K., 1999. Spherical neutron detector for space neutron measurement. *Nucl. Instrum. Methods Phys. Res., Sect. A* 422, 600–605.
- Zhou, B., Li, T., Xu, Y., Gong, C., Yan, Q., Li, L., 2013. Study on method of dose estimation for the dual-moderated neutron survey meter. *Radiat. Meas.* 59, 81–83.